https://ntrs.nasa.gov/search.jsp?R=19680009757 2020-03-24T00:23:16+00:00Z

NASA TECHNICAL NOTE

NASA TN D-4410

C.1

TECH LIBRARY KAFB, NM
0134411

NASA TN D-4410

LOAN COPY: RETURN TO
AFWL (WLIL-2)
KIRTLAND AFB, N MEX

EVALUATION OF LATERAL-DIRECTIONAL HANDLING QUALITIES OF PILOTED REENTRY VEHICLES UTILIZING A FIXED-BASE SIMULATION

by Frank J. van Leynseele

Flight Research Center
Edwards, Calif.

RECEIVED
29 MAR 1968
Technical Library

NATIONAL AERONAUTICS AND SPACE ADMINISTRATION • WASHINGTON, D. C. • MARCH 1968

TECH LIBRARY KAFB, NM
0131341

EVALUATION OF LATERAL-DIRECTIONAL HANDLING QUALITIES OF PILOTED REENTRY VEHICLES UTILIZING A FIXED-BASE SIMULATION

By Frank J. van Leynseele

Flight Research Center
Edwards, Calif.

NATIONAL AERONAUTICS AND SPACE ADMINISTRATION

For sale by the Clearinghouse for Federal Scientific and Technical Information
Springfield, Virginia 22151 – CFSTI price $3.00

EVALUATION OF LATERAL-DIRECTIONAL HANDLING QUALITIES OF PILOTED REENTRY VEHICLES UTILIZING A FIXED-BASE SIMULATION

By Frank J. van Leynseele
Flight Research Center

SUMMARY

A simulator investigation was conducted to evaluate the lateral-directional handling qualities of piloted reentry vehicles. The lateral-directional parameters were chosen to represent a sample of dynamic characteristics typical of reentry-vehicle configurations. The evaluations were made by using a three-degree-of-freedom fixed-base simulator with a pseudo-outside world visual display (contact analog). The investigation showed that the pilots preferred the ratio of the roll transfer function numerator frequency to the Dutch roll frequency to be unity, independent of the magnitude of bank angle to sideslip angle ratio. They objected to an excessive amount of sideslip-angle excitation with ailerons when the ratio of the roll transfer function numerator frequency to the Dutch roll frequency differed from unity, the bank angle to sideslip angle ratio was low, and the yawing moment due to aileron was large.

The evaluation also established that large rolling-motion excursions led to pilot miscoordination when the roll transfer function numerator frequency to Dutch roll frequency was larger than unity and the bank angle to sideslip angle ratio was large.

A comparison of the results obtained with the three-degree-of-freedom contact-analog simulator and results obtained during a related study with a five-degree-of-freedom variable-stability T-33 airplane showed good correlation.

INTRODUCTION

The lateral-directional dynamics of lifting reentry vehicles differ from those of most conventional aircraft in that they are characterized by large dihedral effect, low Dutch roll damping, proverse or adverse aileron yaw, and low roll control power. When the reentry vehicle comes under the influence of atmospheric density, all or a part of the dynamic characteristics can vary rapidly while the pilot navigates the vehicle to a landing site.

Previous studies identified some of the more significant variations of lateral-directional handling-qualities parameters that can be readily perceived by experienced test pilots. In reference 1, a theoretical approach to the pilot closed-loop control of

bank angle by aileron was emphasized. This approach revealed certain combinations of parameters $\left(\frac{\omega_\varphi}{\omega_{DR}}, \frac{1}{\tau_r}, \frac{1}{\tau_s}, \left|\frac{\tau_s}{\tau_r}\right|, \left|\frac{\varphi}{\beta}\right|, \zeta_{DR}, \omega_{DR}\right)$ that led to degradation of piloting performance and, hypothetically, to degraded pilot opinion. An experimental study conducted with a variable-stability airborne simulator was discussed in reference 2. This study investigated the handling qualities of simulated reentry vehicles and confirmed and supplemented some of the results of reference 1. Reference 2 reported that when the roll control parameters were fixed at desirable quantities, the pilot ratings were affected independently by variations of Dutch roll damping ζ_{DR}, the ratio of the roll transfer function numerator to the Dutch roll frequency $\frac{\omega_\varphi}{\omega_{DR}}$, the ratio of roll angle to sideslip angle $\left|\frac{\varphi}{\beta}\right|$, and to a lesser degree by Dutch roll frequency ω_{DR}. However, some of the results of reference 2 were in disagreement with a preliminary investigation made at the NASA Flight Research Center with a fixed-base simulator.

In an effort to obtain a further insight into the controllability provided by the lateral-directional parameters that are representative of reentry vehicles, a program to validate and extend the experimental study reported in reference 2 was undertaken. This program presented a range of dynamic characteristics that was evaluated by two test pilots on three simulators in order to determine the effects of method of simulation on pilot rating and vehicle handling characteristics. The simulators were:

1. A fixed-base three-degree-of-freedom (lateral-directional) analog-computer mechanization equipped with a pseudo-outside world visual display (contact analog).

2. A fixed-base five-degree-of-freedom (velocity invariant) analog-computer mechanization of a T-33 variable-stability airplane with the standard cockpit instruments for display.

3. A five-degree-of-freedom (velocity invariant) flight simulation using the same T-33 variable-stability airplane with the dynamics modified by means of a response feedback system.

A specific objective of this program was to resolve if the most favorable pilot ratings are given for $\frac{\omega_\varphi}{\omega_{DR}}$ near unity or for $\frac{\omega_\varphi}{\omega_{DR}} \approx 0.85$ (adverse yaw) when the bank angle to sideslip angle ratio $\left|\frac{\varphi}{\beta}\right|$ is approximately 9.0 and the Dutch roll damping ratio ζ_{DR} is approximately 0.12. Three values of $\left|\frac{\varphi}{\beta}\right|$ were selected for evaluation, 0.67, 9.2, and 13.0. The first and second values permitted direct correlation with the results of reference 2; the third value extended the scope of the subject study. The lowest $\left|\frac{\varphi}{\beta}\right|$ value provided a baseline reference representative of existing aircraft; whereas, the higher $\left|\frac{\varphi}{\beta}\right|$ values were representative of reentry vehicles.

This program was a joint technical effort by Cornell Aeronautical Laboratory and the NASA Flight Research Center. The work was sponsored by the Flight Research Center and performed by the Flight Research Department of Cornell Aeronautical Laboratory under contract with the Air Force Flight Dynamics Laboratory. The fixed-base evaluations with the T-33 airplane were performed at Buffalo, N. Y., and the in-flight (T-33) and fixed-base (contact analog) evaluations at Edwards, Calif.

This paper presents the results obtained with the fixed-base three-degree-of-freedom simulation equipped with a contact-analog visual display and compares these results with results from the other simulations. The results obtained with the ground and in-flight T-33 variable-stability airplane are discussed in detail in reference 3.

SYMBOLS

g — acceleration of gravity, ft/sec^2 (m/sec^2)

$j = \sqrt{-1}$

$j\omega$ — designation of imaginary axis of s-plane

I_X — moment of inertia about X-axis, slug-ft^2 (kg-m^2)

I_{XZ} — product of inertia, slug-ft^2 (kg-m^2)

I_Z — moment of inertia about Z-axis, slug-ft^2 (kg-m^2)

$k = \dfrac{1}{1 - \dfrac{I_{XZ}^2}{I_X I_Z}}$

L — rolling moment, ft-lb (m-kg)

$L_p = \dfrac{1}{I_X}\dfrac{\partial L}{\partial p}, \dfrac{1}{\text{sec}}$

$L'_p = k\left(L_p + \dfrac{I_{XZ}}{I_X} N_p\right), \dfrac{1}{\text{sec}}$

$$L_r = \frac{1}{I_X}\frac{\partial L}{\partial r}, \frac{1}{sec}$$

$$L'_r = k\left(L_r + \frac{I_{XZ}}{I_X}N_r\right), \frac{1}{sec}$$

$$L_\beta = \frac{1}{I_X}\frac{\partial L}{\partial \beta}, \frac{1}{sec^2}$$

$$L'_\beta = k\left(L_\beta + \frac{I_{XZ}}{I_X}N_\beta\right), \frac{1}{sec^2}$$

$$L_{\delta_a} = \frac{1}{I_X}\frac{\partial L}{\partial \delta_a}, \frac{1}{sec^2}$$

$$L_{\delta_{a_s}} = L_{\delta_a}\left(\frac{\delta_a}{\delta_{a_s}}\right), \frac{1}{sec^2\text{-in.}} \left(\frac{1}{sec^2\text{-cm}}\right)$$

$$L'_{\delta_{a_s}} = k\left(L_{\delta_{a_s}} + \frac{I_{XZ}}{I_X}N_{\delta_{a_s}}\right), \frac{1}{sec^2\text{-in.}} \left(\frac{1}{sec^2\text{-cm}}\right)$$

$$L_{\delta_r} = \frac{1}{I_X}\frac{\partial L}{\partial \delta_r}, \frac{1}{sec^2}$$

$$L_{\delta_{r_p}} = L_{\delta_r}\left(\frac{\delta_r}{\delta_{r_p}}\right), \frac{1}{sec^2\text{-in.}} \left(\frac{1}{sec^2\text{-cm}}\right)$$

$$L'_{\delta_{r_p}} = k\left(L_{\delta_{r_p}} + \frac{I_{XZ}}{I_X}N_{\delta_{r_p}}\right), \frac{1}{sec^2\text{-in.}} \left(\frac{1}{sec^2\text{-cm}}\right)$$

m mass, slugs (kg)

N yawing moment, ft-lb (m-kg)

$$N_p = \frac{1}{I_Z}\frac{\partial N}{\partial p}, \frac{1}{sec}$$

$$N'_p = k\left(N_p + \frac{I_{XZ}}{I_Z} L_p\right), \frac{1}{sec}$$

$$N_r = \frac{1}{I_Z}\frac{\partial N}{\partial r}, \frac{1}{sec}$$

$$N'_r = k\left(N_r + \frac{I_{XZ}}{I_Z} L_r\right), \frac{1}{sec}$$

$$N_\beta = \frac{1}{I_Z}\frac{\partial N}{\partial \beta}, \frac{1}{sec^2}$$

$$N'_\beta = k\left(N_\beta + \frac{I_{XZ}}{I_Z} L_\beta\right), \frac{1}{sec^2}$$

$$N_{\delta_a} = \frac{1}{I_Z}\frac{\partial N}{\partial \delta_a}, \frac{1}{sec^2}$$

$$N_{\delta_{a_s}} = N_{\delta_a}\left(\frac{\delta_a}{\delta_{a_s}}\right), \frac{1}{sec^2\text{-in.}} \left(\frac{1}{sec^2\text{-cm}}\right)$$

$$N'_{\delta_{a_s}} = k\left(N_{\delta_{a_s}} + \frac{I_{XZ}}{I_Z} L_{\delta_{a_s}}\right), \frac{1}{sec^2\text{-in.}} \left(\frac{1}{sec^2\text{-in.}}\right)$$

$$N_{\delta_r} = \frac{1}{I_Z}\frac{\partial N}{\partial \delta_r}, \frac{1}{sec^2}$$

$$N_{\delta_{r_p}} = N_{\delta_r}\left(\frac{\delta_r}{\delta_{r_p}}\right), \frac{1}{sec^2\text{-in.}} \left(\frac{1}{sec^2\text{-cm}}\right)$$

$$N'_{\delta_{r_p}} = k\left(N_{\delta_{r_p}} + \frac{I_{XZ}}{I_Z} L_{\delta_{r_p}}\right), \frac{1}{sec^2\text{-in.}} \left(\frac{1}{sec^2\text{-in.}}\right)$$

p roll rate, rad/sec

p_{ss} steady-state roll rate, rad/sec

r yaw rate, rad/sec

s Laplace transform operator

t time, sec

V true velocity, ft/sec (m/sec)

X, Z force components in the stability-axes system; the X-axis is alined with the relative wind at zero sideslip in trimmed flight; Z-axis is in the plane of symmetry

Y side force, lb (kg)

$Y_\beta = \frac{1}{mV}\frac{\partial Y}{\partial \beta}, \frac{1}{sec}$

$Y_{\delta_a} = \frac{1}{mV}\frac{\partial Y}{\partial \delta_a}, \frac{1}{sec}$

$Y_{\delta_{a_s}} = Y_{\delta_a}\left(\frac{\delta_a}{\delta_{a_s}}\right), \frac{1}{sec\text{-}in.}\ \left(\frac{1}{sec\text{-}cm}\right)$

$Y_{\delta_r} = \frac{1}{mV}\frac{\partial Y}{\partial \delta_r}, \frac{1}{sec}$

$Y_{\delta_{r_p}} = Y_{\delta_r}\left(\frac{\delta_r}{\delta_{r_p}}\right), \frac{1}{sec\text{-}in.}\ \left(\frac{1}{sec\text{-}cm}\right)$

β angle of sideslip, rad

δ_a aileron surface deflection, positive when right aileron trailing edge is deflected upward, rad

δ_{a_s} aileron stick deflection, positive when stick is deflected to the right, in. (cm)

δ_r rudder surface deflection, positive when rudder surface is deflected to the left, rad

δ_{r_p}	rudder pedal deflection, positive when left pedal is pushed forward, in. (cm)
ζ_{DR}	Dutch roll damping ratio
ζ_{φ}	damping ratio of numerator quadratic in roll to aileron input transfer function
σ	designation of real axis of s-plane
τ_r	roll-mode time constant, sec
τ_s	spiral-mode time constant, sec
φ	bank angle, rad
ω_{DR}	Dutch roll undamped natural frequency, rad/sec
ω_{φ}	undamped natural frequency of numerator quadratic in roll to aileron input transfer function, rad/sec
$\|\|$	absolute value

A dot over a quantity indicates the differentiation with respect to time.

APPARATUS

The evaluation was performed by using a simplified fixed-base cockpit mechanized with a general-purpose analog computer (fig. 1). The analog computer was mechanized to solve the three-degree-of-freedom lateral-directional small-perturbation equations of motion presented in appendix A.

The cockpit was equipped with rudder pedals, control stick, instrument panel, and contact-analog display. The stick and rudder-pedal movements were converted to dc electrical signals by linear position transducers. The signals were used as inputs to the analog computer equations of motion.

The stick and rudder-pedal bungees provided force proportional to the displacement of the controls, thus simulating a linear force feel system. The control displacement,

force gradients, and gearing used in the contact-analog simulator were as follows:

Controller	Axes	Displacement,		Force gradient,		Gearing, deg/in.
		in.	cm	lb/in.	kg/cm	
Stick	Lateral	±3.00*	±7.62	4.67	0.834	2.86
Pedal	Directional	±3.25	±8.25	16.30	2.91	----

*Dimensions measured at a handgrip point 3.30 in. (8.38 cm) from the top of the stick.

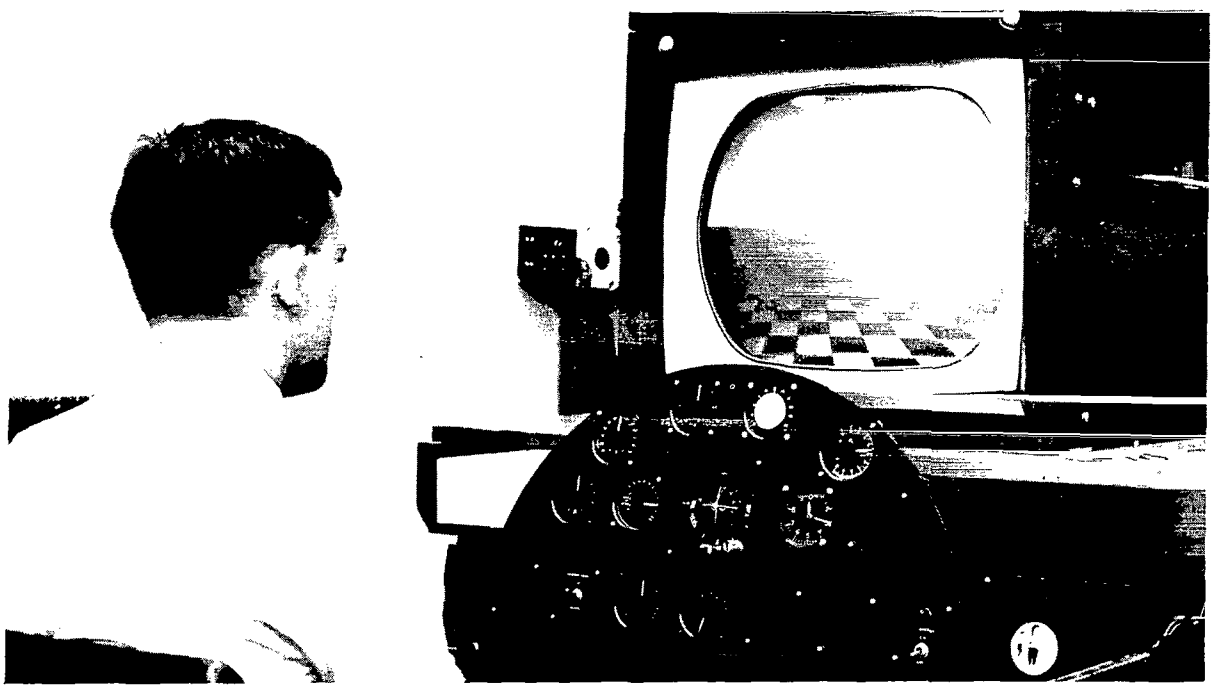

E- 12943

Figure 1.– Cockpit and contact analog.

The pilot observed the simulated aircraft motions through a contact-analog visual system augmented by an attitude indicator (Lear, Inc., Model 40-60-C, 5-in. (12.70-cm) diameter) driven by dc servo synchros commanded by the analog computer. The pitch axis was not mechanized for this simulation. Additional sideslip information was available through a β-meter, which was a dc voltmeter with a 3-inch (7.62-centimeter) diameter black dial. The 12 o'clock position was calibrated for zero sideslip angle, with 0.5° increments. Each degree mark was accentuated, for a total of 5° left and right of center.

The contact-analog display system generated its own symbols: moving foreground pattern, sky with cloud patterns, horizon line, and fixed cross. These images were projected onto a 21-inch color-television tube positioned at eye level 3 feet to 3.5 feet (0.914 meter to 1.067 meters) in front of the pilot and above the instrument panel. At the center of the television screen a fixed cross represented the airplane. The motion

of the images surrounding the cross was the result of the analog-computer output and showed the response to the pilot inputs.

There was no transport time lag in the presentation. In brief, the contact-analog display presented a qualitative view of the aircraft's motion that was similar to viewing aircraft motions through a cockpit windshield, hence, a pseudo-outside world display.

The results presented from reference 3 were obtained with a T-33 jet trainer that had been extensively modified. A detailed description of this airplane is given in references 4 to 6.

PILOT INSTRUCTIONS

The evaluation pilots, one from Cornell Aeronautical Laboratory (pilot A) and one from the Flight Research Center (pilot B), were experienced engineering test pilots with a background in handling-qualities evaluation. They were briefed on the following ground rules, devised to give them an understanding of the basis for rating the configurations:

1. The overall mission was to control a reentry vehicle from hypersonic flight at high altitude, through subsonic flight, to a conventional aircraft-type landing.

2. The controlling task did not require high maneuverability but did require fairly precise control of attitude. Each configuration was to be evaluated in light of the entire mission, keeping in mind that the evaluation was restricted to a three-degree-of-freedom lateral-directional simulation.

3. The evaluation comments and ratings were to be based primarily on visual flying using a pseudo-outside world display (contact analog) supplemented by attitude and sideslip indicators.

The following required piloting tasks were defined with the collaboration of the evaluation pilots:

1. Straight flight, including small turns with a heading change of less than 30°.

2. Turning flight, including shallow (up to 30°) and medium (up to 60°) banked turns involving heading changes of at least 90°, with particular attention to the control of nose position with bank angle.

3. Rolling flight, including slow and rapid rolling maneuvers, and 180° rolls when handling characteristics permitted.

In addition to the prescribed tasks, the pilots were encouraged to perform supplemental maneuvers at their discretion. Pilot comments resulting from the evaluation of a flight condition were immediately recorded on a voice tape recorder and later typed and edited. The following "comment card" was given to the pilots in an attempt to evoke pertinent comments.

PILOT COMMENT CARD

I. Make "general comments" as desired.

II. Following maneuvers performed under piloting task, comment on:

(1) Pilot's Control
  (a) Aileron : Feel-response to aileron inputs
  (b) Rudder : Feel-response to rudder inputs

(2) Roll Control : Ability to maintain bank angle
Ability to change bank angle
Any special techniques used

(3) Heading Control: Ability to maintain heading
Ability to change heading
Any special techniques used

(4) Interactions
  (a) Control : Roll due to rudder
Yaw due to aileron
  (b) Response : Roll due to sideslip
Yaw due to roll rate

III. Following the completion of the maneuvers:

(1) Summarize major objections and/or favorable features

(2) Comment on primary instruments and visual cues used

(3) Comment on any special piloting techniques required

(4) Assign numerical and adjective rating

(5) Comment on adequacy of simulation

Finally, the pilot was requested to assign a numerical rating for each evaluation based on the modified Cooper Scale shown below:

Category	Adjective description within category		Numerical rating
	Satisfactory	Excellent	1
		Good	2
		Fair	3
Acceptable ------ (ask that it be fixed) ----------			
	Unsatisfactory	Fair	4
		Poor	5
		Bad	6
---------- (won't buy it) ----------			
	Flyable	Bad	7
		Very bad	8
		Dangerous	9
Unacceptable --------- (won't fly it) ----------			
	Unflyable	Unflyable	10

7 - Required major portion of pilot's attention
8 - Controllable only with a minimum of cockpit duties
9 - Aircraft just controllable with complete attention

No information was given the pilots regarding the random appearing changes in parameters from one configuration to the next. The pilots were instructed not to discuss their findings between themselves but were encouraged to discuss problems with the Project Engineer.

PARAMETERS INVESTIGATED

The derivatives and dynamics simulated were as follows:

Configuration	ω_{DR}, rad/sec	ζ_{DR}	$\frac{\omega_\varphi}{\omega_{DR}}$	ζ_φ	$\left\|\frac{\varphi}{\beta}\right\|$	τ_r, sec	τ_s, sec	$\frac{p_{ss}}{\delta_{a_s}}$, rad/sec-in.	$\frac{p_{ss}}{\delta_{a_s}}$, rad/sec-cm	L'_β, rad/sec^2	N'_β, rad/sec^2	$L'_{\delta_{a_s}}$, rad/sec^2-in.	$L'_{\delta_{a_s}}$, rad/sec^2-cm	$N'_{\delta_{a_s}}$, rad/sec^2-in.	$N'_{\delta_{a_s}}$, rad/sec^2-cm
1	2.30	0.103	0.93	0.111	0.67	0.39	270	0.323	0.127	-5.36	5.16	0.954	0.375	-0.120	-0.0473
2	2.30	.103	.99	.110	.67	.39	270	.299	.118	-5.36	5.16	.782	.308	-.0067	-.00263
3	2.30	.103	1.05	.110	.67	.39	270	.294	.116	-5.36	5.16	.685	.269	.083	.0326
4	2.17	.177	.575	.206	9.2	.33	11.4	.142	.056	-77.1	4.91	1.307	.514	-.048	-.0189
5	2.17	.177	.830	.154	9.2	.33	11.4	.247	.0973	-77.1	4.91	1.09	.429	-.0245	-.00964
6	2.17	.177	1.03	.143	9.2	.33	11.4	.301	.118	-77.1	4.91	.861	.339	.00039	.000153
7	2.17	.177	1.11	.123	9.2	.33	11.4	.287	.113	-77.1	4.91	.706	.278	.0097	.00382
8	2.17	.177	1.47	.194	9.2	.33	11.4	.135	.0531	-77.1	4.91	.190	.0749	.0734	.0288
9	2.30	.130	.85	.124	13.0	.37	10^6	.355	.1395	-102.2	5.67	1.34	.527	-.0255	-.00100
10	2.30	.130	1.0	.133	13.0	.37	10^6	.360	.1417	-102.2	5.67	.974	.383	-.00426	-.00167
11	2.30	.130	1.15	.145	13.0	.37	10^6	.359	.141	-102.2	5.67	.735	.289	.0080	.00315
12	2.30	.130	1.25	.162	13.0	.37	10^6	.322	.1265	-102.2	5.67	.558	.219	.0171	.00673
13	2.30	.130	1.59	.197	13.0	.37	10^6	.304	.119	-102.2	5.67	.325	.128	.0276	.01088

The ratio of the roll transfer function numerator frequency to the Dutch roll frequency $\frac{\omega_\varphi}{\omega_{DR}}$ was varied from 0.575 to 1.59 to provide a measure of roll disturbance at Dutch roll frequency due to aileron inputs. The ratio reflects adverse $\left(\frac{\omega_\varphi}{\omega_{DR}} < 1.0\right)$ or proverse $\left(\frac{\omega_\varphi}{\omega_{DR}} > 1.0\right)$ yaw due to aileron.

The ratio of bank angle to sideslip angle $\left|\frac{\varphi}{\beta}\right|$ was evaluated at three magnitudes (0.67, 9.2, and 13.0). The significant derivatives were L'_β and N'_β, where N'_β remained essentially constant. Only negative L'_β values were investigated.

For a given value of $\left|\frac{\varphi}{\beta}\right|$, the Dutch roll frequency ω_{DR} and damping ζ_{DR}, and roll mode τ_r and spiral mode τ_s time constants were invariant.

In order to vary the $\frac{\omega_\varphi}{\omega_{DR}}$ ratio with ω_{DR} remaining constant, it was necessary to increase or decrease the numerator frequency ω_φ. This was achieved by varying the yawing moment due to aileron $N'_{\delta_{a_s}}$, including positive and negative values.

To maintain an acceptable level of steady-state roll rate per aileron stick displacement while $\frac{\omega_\varphi}{\omega_{DR}}$ was varied, it was necessary to adjust the rolling moment due to aileron derivative $L'_{\delta_{a_s}}$, inasmuch as $p_{ss} = \tau_r L'_{\delta_{a_s}} \left(\frac{\omega_\varphi}{\omega_{DR}}\right)^2$. By varying $L'_{\delta_{a_s}}$,

the numerator damping ζ_{φ} was varied by a small amount. Also, by increasing $L'_{\delta_{a_s}}$ for the adverse aileron yaw and decreasing it for the proverse aileron yaw, the initial roll acceleration was affected.

RESULTS AND DISCUSSION

The results of this study are summarized as pilot ratings of the configurations evaluated. These ratings represent an overall measure of the acceptability of the handling qualities for the task defined. Pilot comments and computed responses for the various configurations are analyzed in order to provide insight into the particular difficulties encountered and to indicate the reasons for the undesirable handling qualities. In addition, the effectiveness of the piloting techniques used is discussed.

Pilot Opinion Data

Low bank angle to sideslip angle ratio $\left(\left|\frac{\varphi}{\beta}\right| = 0.67\right)$. – Figure 2 is a plot of pilot rating versus $\frac{\omega_{\varphi}}{\omega_{DR}}$ for $\left|\frac{\varphi}{\beta}\right| = 0.67$ and low Dutch roll damping $\zeta_{DR} = 0.103$. The average ratings of pilot A and pilot B are presented as curves and show good agreement in trend.

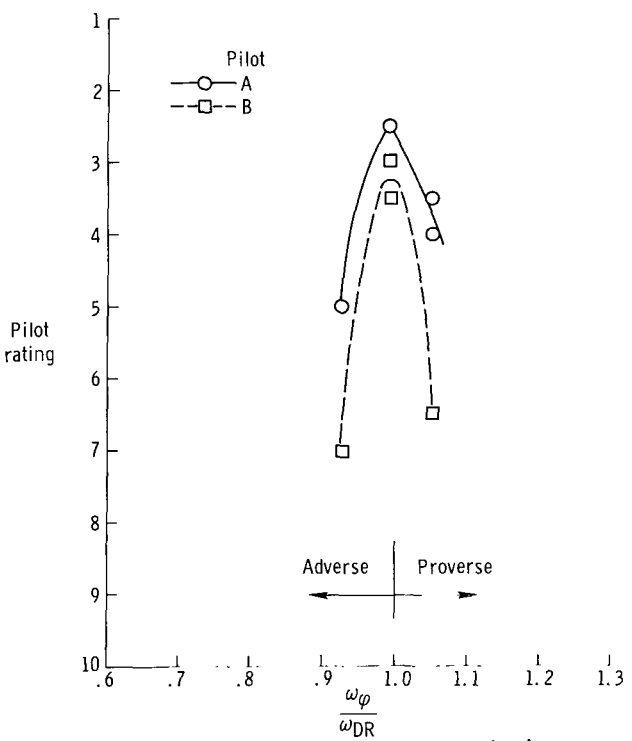

Figure 2.– Comparison of pilot rating trends. $\left|\frac{\varphi}{\beta}\right| = 0.67$; $\zeta_{DR} = 0.103$.

In general, both pilots degraded the configurations in proportion to the amount of sideslip oscillation induced by aileron control inputs. The most favorable ratings were for values of $\frac{\omega_{\varphi}}{\omega_{DR}}$ near unity with small values of $N'_{\delta_{a_s}}$.

The aileron-induced sideslip was the predominant deterrent to satisfactory control. For adverse aileron yaw $\left(\frac{\omega_{\varphi}}{\omega_{DR}} = 0.93\right)$ and proverse aileron yaw $\left(\frac{\omega_{\varphi}}{\omega_{DR}} = 1.05\right)$ the Dutch roll excitation was sensitive to rapid aileron application or large rolling maneuvers or both. The Dutch roll oscillations were notably reduced when the pilots used smaller or slower aileron inputs or both, thus, in effect, decreasing the pilot's gain.

Because it was small, the positive dihedral effect L'_β had a minor effect on bank-angle oscillations. The use of small or slow aileron inputs or both produced lower-amplitude oscillations in bank angle than did large or rapid aileron inputs. The roll rate, roll sensitivity, and bank-angle control were not appreciably affected by the $\frac{\omega_\varphi}{\omega_{DR}}$ variations.

The flight-path heading control was rated acceptable but with deficiencies. A precise flight-path heading control was lacking for $\frac{\omega_\varphi}{\omega_{DR}} = 0.93$ and 1.05. The rating for $\frac{\omega_\varphi}{\omega_{DR}} = 0.99$ was "satisfactory." Heading control was better with proverse yaw than with adverse yaw where there was a tendency to roll out on heading too late. Adverse yaw allowed better control of Dutch roll oscillations when rudders and the $\dot{\beta}$ technique were used to damp the oscillations. These techniques are discussed later in more detail in the Remarks on Pilot Techniques section.

High bank angle to sideslip angle ratio $\left(\left|\frac{\varphi}{\beta}\right| = 9.2\right)$. – Figure 3 is a plot of pilot rating versus $\frac{\omega_\varphi}{\omega_{DR}}$ for $\left|\frac{\varphi}{\beta}\right| = 9.2$ and Dutch roll damping of $\zeta_{DR} = 0.177$. The average ratings of pilot A and pilot B show good agreement in trend. The agreement

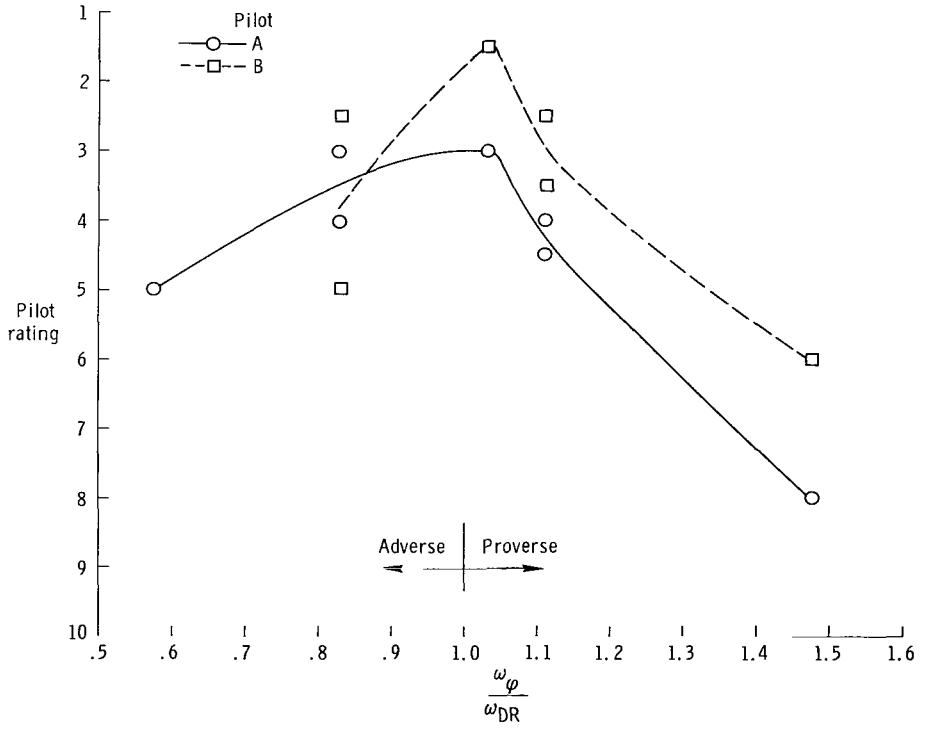

Figure 3.– Comparison of pilot rating trends. $\left|\frac{\varphi}{\beta}\right| = 9.2$; $\zeta_{DR} = 0.177$.

became even more apparent when the pilot comments were analyzed. The critiques of the bothersome modes and the special techniques used to control the configurations showed remarkable similarity.

In general, the major deterrent to satisfactory control of these configurations was the excessive amount of roll due to sideslip with the consequent miscoordination in bank-angle control.

Adverse yaw: Under adverse yaw conditions the pilots found the roll rate response to be "jerky" and the Dutch roll excitation to be proportional to the amount of adverse yaw. For $\frac{\omega_\varphi}{\omega_{DR}} = 0.575$ the magnitude of the oscillations in roll rate indicated apparent roll control reversal when large or sharp aileron inputs or both were used. The magnitude of the roll oscillations was smaller when slower or smaller aileron inputs or both were used. The large dihedral effect ($L'_\beta = -77.1$) caused the aileron-induced sideslip to produce large rolling motion.

Proverse yaw: The most favorable ratings were for proverse yaw at $\frac{\omega_\varphi}{\omega_{DR}} = 1.03$. The aileron inputs produced very little sideslip, and bank-angle control was good. The onset of a pilot-induced oscillation (PIO) occurred at $\frac{\omega_\varphi}{\omega_{DR}} = 1.11$. The pilots noted a decrease in effective closed-loop damping. The largest proverse yaw $\left(\frac{\omega_\varphi}{\omega_{DR}} = 1.47\right)$ produced a marked increase in the tendency for pilot-induced oscillations. Aileron control inputs induced yawing motions, and the large effective dihedral produced rolling oscillations. A noticeable lag in roll-rate initiation and a decreased roll acceleration contributed to the problem. The use of slow and small aileron applications enabled the pilots to control the roll attitude of the airplane at the cost of an ever-present residual oscillation.

Very high bank angle to sideslip angle ratio $\left(\left|\frac{\varphi}{\beta}\right| = 13.0\right)$. – Figure 4 is a plot of pilot rating versus $\frac{\omega_\varphi}{\omega_{DR}}$ for $\left|\frac{\varphi}{\beta}\right| = 13.0$ and $\zeta_{DR} = 0.13$. The average ratings of pilots A and B show good agreement. Generally, the configurations with $\left|\frac{\varphi}{\beta}\right| = 13.0$ exhibited behavior similar to that of the previously discussed $\left|\frac{\varphi}{\beta}\right| = 9.2$ configurations (fig. 3).

Adverse yaw: Both pilots rated $\frac{\omega_\varphi}{\omega_{DR}} = 0.85$ "satisfactory" (PR = 3.0). When $\frac{\omega_\varphi}{\omega_{DR}} = 1.0$ each pilot gave his most favorable rating. Little or no yaw due to aileron was produced, even with large and rapid aileron inputs. The value of $N'_{\delta_{as}}$ was small.

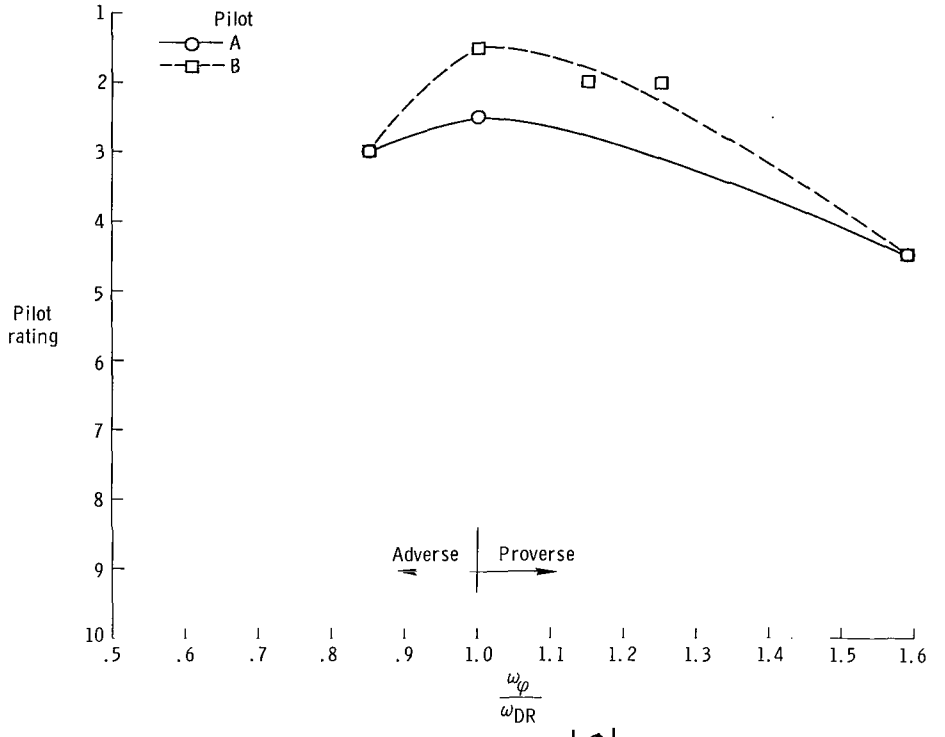

Figure 4.– Comparison of pilot rating trends. $\left|\frac{\varphi}{\beta}\right| = 13.0$; $\zeta_{DR} = 0.13$.

Proverse yaw: Both pilots gave the large proverse yaw $\left(\frac{\omega_\varphi}{\omega_{DR}} = 1.59\right)$ a pilot rating of 4.5. The pilots objected to the roll oscillations, as shown by the following quote from the pilot comments:

> "...while performing rolling maneuvers using large and abrupt aileron inputs, the magnitudes of the Dutch roll oscillations were large. The sideslip angle oscillations (±2° of β) coupled with a bothersome bank angle oscillation. Bank angle control was poor. The pilot had to work constantly to stay within ±10° of the desired bank angle. The bank angle oscillations were present whether flying wings level or performing shallow banked turns."

As expected, when small and slow aileron inputs were used, the pilot-induced oscillations decreased to the point of reasonable controllability with the aid of considerable pilot compensation.

Experimental Data

Figure 5 is a plot of the combined average pilot ratings for pilots A and B versus $\frac{\omega_\varphi}{\omega_{DR}}$ for three values of $\left|\frac{\varphi}{\beta}\right|$ (0.67, 9.2, and 13.0). Also shown are results for two comparable conditions obtained from reference 2; these evaluations were made by

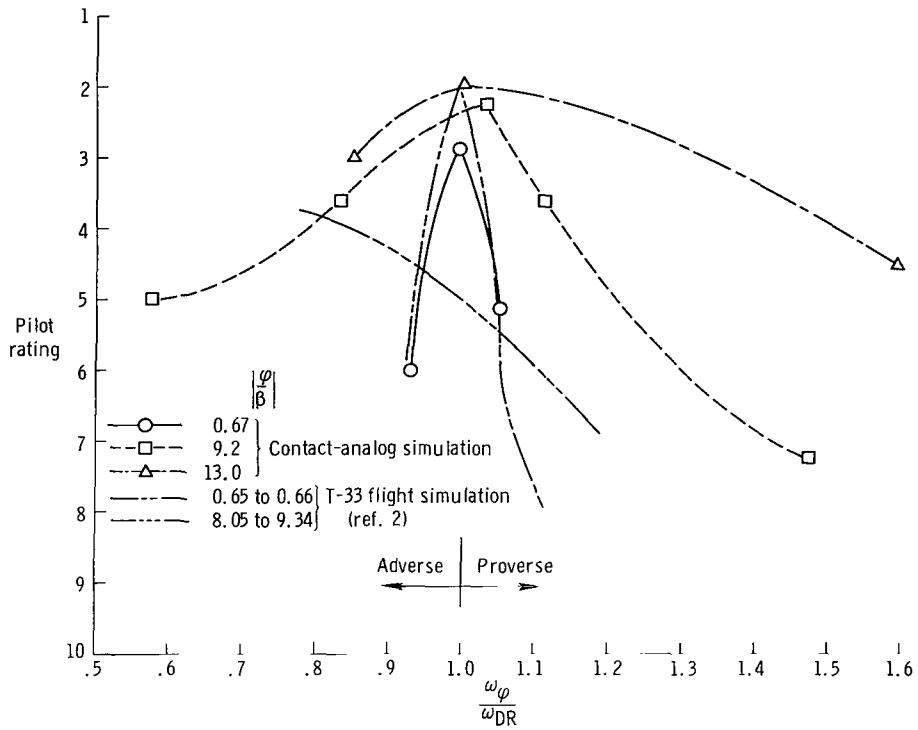

Figure 5.– Pilot rating versus $\frac{\omega_\varphi}{\omega_{DR}}$ at various ratios of $\left|\frac{\varphi}{\beta}\right|$.

pilot A using the variable-stability T-33 airplane. The curve for $\left|\frac{\varphi}{\beta}\right| = 0.65$ to 0.66 from reference 2 is included for comparison with the contact-analog-simulation results of $\left|\frac{\varphi}{\beta}\right| = 0.67$. Good correlation exists between the two curves. The curve for $\left|\frac{\varphi}{\beta}\right| = 8.05$ to 9.34 from reference 2 is discussed in a later section.

Yaw due to aileron effect. – In figure 5 the low $\left|\frac{\varphi}{\beta}\right|$ curve (0.67) shows a sharp drop in pilot rating for small incremental changes in $\frac{\omega_\varphi}{\omega_{DR}}$ from a value of 1.0. The high $\left|\frac{\varphi}{\beta}\right|$ curves (9.2 and 13.0) did not show the same tendency. The following approximate expression for $\frac{\omega_\varphi}{\omega_{DR}}$ is presented in order to explain the changes to the dominant derivatives when the $\left|\frac{\varphi}{\beta}\right|$ ratio was varied:

$$\frac{\omega_\varphi}{\omega_{DR}} = \left[1 - \left(\frac{N'\delta_{a_S}}{L'\delta_{a_S}}\right)\left(\frac{L'_\beta}{N'_\beta}\right)\right]^{1/2}$$

The derivation and simplification of this expression are presented in appendix B. It should be noted that the exact expression was used for data analysis, whereas the simplified expression is used in the following discussion.

When $\frac{\varphi}{\beta}$ was small, so was $\left|\frac{L'_\beta}{N'_\beta}\right|$. In order to vary $\frac{\omega_\varphi}{\omega_{DR}}$ incrementally, $\left|\frac{N'_{\delta_{a_s}}}{L'_{\delta_{a_s}}}\right|$ had to be varied an appreciable amount, with the added constraint that $L'_{\delta_{a_s}}$ was a term in the $\frac{p_{ss}}{\delta_{a_s}}$ transfer function that was maintained at a desirable level. Thus, the yawing moment due to aileron $\left|N'_{\delta_{a_s}}\right|$ had to be significantly increased.

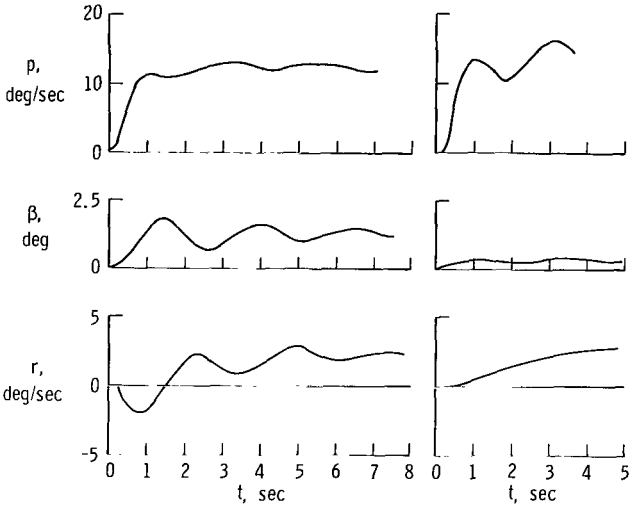

(a) Configuration 1 (table, p. 11); PR = 6.0.

(b) Configuration 9 (table, p. 11); PR = 3.0.

Figure 6.– Time histories showing the effect of yawing moment due to aileron on the response of two configurations to aileron step inputs.

Figure 6 shows two time histories, one representing large $N'_{\delta_{a_s}}$ (-0.120) and low $\left|\frac{\varphi}{\beta}\right|$ (0.67) (fig. 6(a), configuration 1) and the other representing small $N'_{\delta_{a_s}}$(-0.0255) and high $\left|\frac{\varphi}{\beta}\right|$ (13.0) (fig. 6(b), configuration 9). It can be seen that when $N'_{\delta_{a_s}}$ was large, large sideslip and yaw-rate oscillations resulted. The pilots disliked the presence of the high values of aileron yaw and rated vehicle controllability at 6.0. When $N'_{\delta_{a_s}}$ was small and $\left|\frac{\varphi}{\beta}\right|$ was large, large-amplitude oscillations in roll rate and small oscillations in sideslip angle and yaw rate were experienced. The average pilot rating was 3.0.

Rolling moment due to sideslip effect. – Because of the large dihedral effect (L'_β = -77.1 and -102.2) associated with the high $\left|\frac{\varphi}{\beta}\right|$ ratios (9.2 and 13.0, respectively), the primary deterrent to control was the excessive roll due to sideslip with the consequent miscoordination in bank-angle control for large adverse or proverse aileron yaw. The large adverse yaw was down-rated by the pilots because of apparent roll reversal; the large proverse yaw resulted in pilot-induced oscillations.

In figure 7(a) it can be seen that configuration 4, which had a large $L'_{\delta_{a_s}}$ (1.307) experienced a rapid initial roll response, and the yawing moment due to aileron ($N'_{\delta_{a_s}}$ = -0.048) and associated large adverse yaw $\left(\frac{\omega_\varphi}{\omega_{DR}} = 0.575\right)$ caused a large-amplitude steady-state oscillation in roll rate. The lightly damped oscillatory response precluded precise bank-angle control, and the pilot's rating was 5.0. In comparison, for configuration 8, which had a large positive value of yawing moment due to aileron

($N'_{\delta_{a_s}} = 0.0734$), an associated proverse yaw $\left(\frac{\omega_\varphi}{\omega_{DR}} = 1.47\right)$, and a smaller value of $L'_{\delta_{a_s}}$ (0.19), the initial roll rate was less rapid (fig. 7(b)); however, the steady-state oscillatory roll response was downrated to 7.25 by the pilots because of their inability to control bank angle precisely.

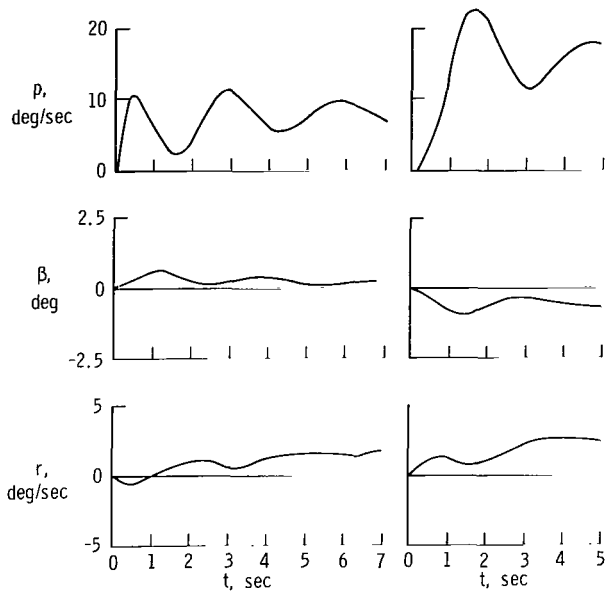

(a) Configuration 4 (table, p, 11); PR = 5.0.

(b) Configuration 8 (table, p. 11); PR = 7.25.

Figure 7.– Time histories showing the effect of adverse and proverse aileron yaw on the response of two configurations to aileron step inputs.

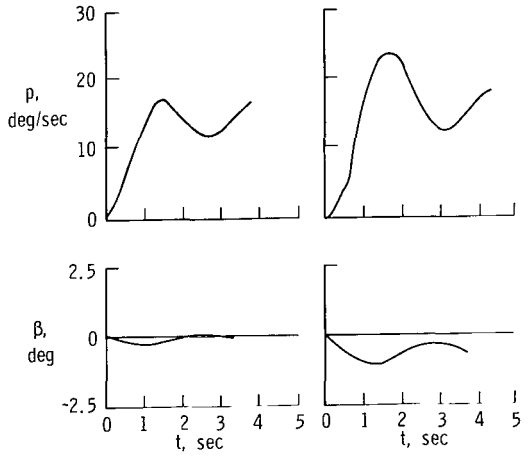

(a) Configuration 13 (table, p. 11); PR = 4.5.

(b) Configuration 8 (table, p. 11); PR = 7.25.

Figure 8.– Time histories showing the effects of yawing moment due to aileron on two proverse aileron yaw responses.

Figure 5 shows that there is good agreement between the $\left|\frac{\varphi}{\beta}\right| = 9.2$ and 13.0 curves for the values of adverse yaw evaluated; however, for the proverse yaw curves, a better overall rating was noted at the highest $\left|\frac{\varphi}{\beta}\right|$ (13.0). An explanation of the different ratings is offered in figures 8(a) and 8(b), which show time histories of the largest values of proverse-yaw responses tested for $\left|\frac{\varphi}{\beta}\right| = 13.0$ and 9.2 ($\frac{\omega_\varphi}{\omega_{DR}} = 1.59$ and 1.47, respectively). The time histories show that an aileron step input produced larger sideslip excitation, a larger roll oscillation, and an unacceptable rating (average rating, 7.25) for $\left|\frac{\varphi}{\beta}\right| = 9.2$. The $\left|\frac{\varphi}{\beta}\right| = 13.0$ condition was rated an acceptable 4.5 even though $\frac{\omega_\varphi}{\omega_{DR}}$ ratio was higher (1.59 compared to 1.47). The fact that $N'_{\delta_{a_s}}$ in figure 8(b) was about three times as large as $N'_{\delta_{a_s}}$ in figure 8(a) was the primary cause of the larger sideslip response and, hence, a larger amplitude roll oscillation.

The configuration was susceptible to pilot-induced oscillations when $\frac{\omega_\varphi}{\omega_{DR}}$ was larger than unity and the rolling moment due to aileron was large. To illustrate

the interaction of the dynamic modes leading to a pilot-induced oscillation, root-locus diagrams are presented in figures 9 and 10. Figure 9 shows the root-locus diagram

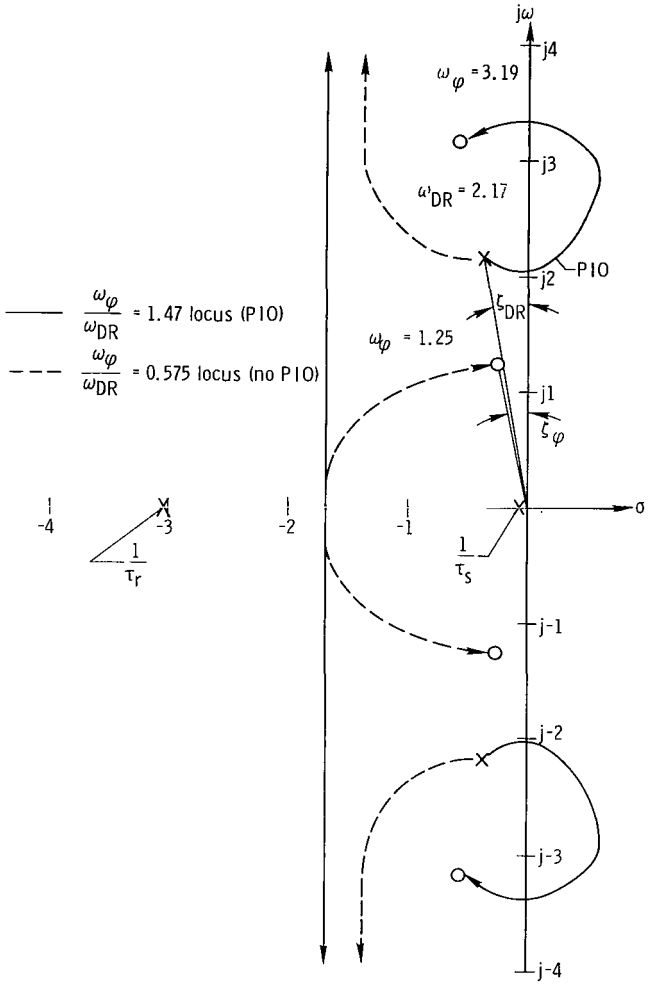

Figure 9.— Root-locus diagram showing the closure of the aileron to bank angle loop for a high bank angle to sideslip angle ratio.

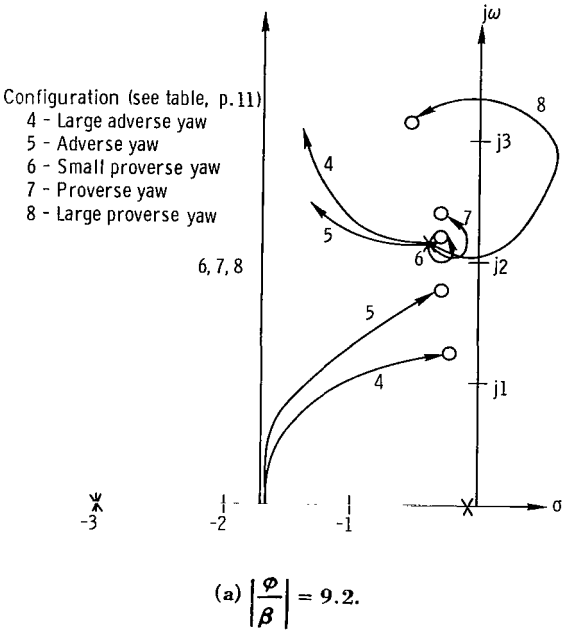

(a) $\left|\frac{\varphi}{\beta}\right| = 9.2.$

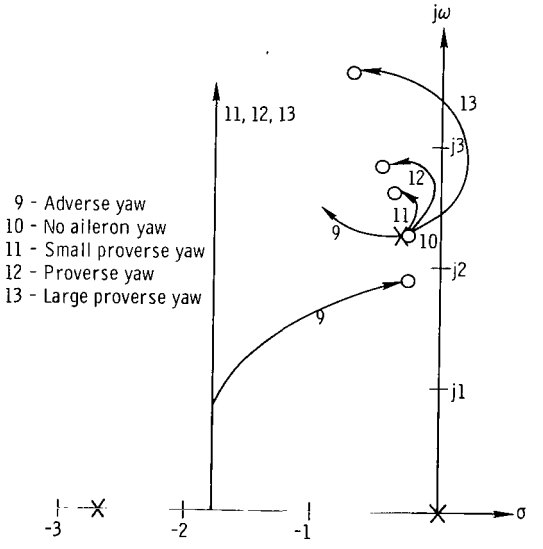

(b) $\left|\frac{\varphi}{\beta}\right| = 13.0.$

Figure 10.— Root-locus diagrams showing the closure of the aileron to bank angle loop for high bank angle to sideslip angle ratio.

of the pilot gain closure of aileron to bank angle loop and illustrates the pilot-induced-oscillation tendency for proverse yaw at high $\left|\frac{\varphi}{\beta}\right|$. It can be seen that the locus of the proverse yaw case (configuration 8, solid lines) $\left(\frac{\omega_\varphi}{\omega_{DR}} = 1.47\right)$ extended into the right-hand plane and the severity of the closed-loop instability depended on the amount of the pilot gain. The adverse yaw case (configuration 4, dashed lines) $\left(\frac{\omega_\varphi}{\omega_{DR}} = 0.575\right)$ did not exhibit closed-loop instability.

Figures 10(a) and 10(b) show root-locus diagrams for the high $\left|\frac{\varphi}{\beta}\right|$ configurations evaluated. For proverse yaw $\left(\frac{\omega_\varphi}{\omega_{DR}} > 1\right)$ the effective closed-loop damping was decreased as a function of $\frac{\omega_\varphi}{\omega_{DR}}$ and pilot gain. The pilots experienced difficulties in maintaining precise bank-angle control for closed-loop bank-angle control with aileron.

In figure 5 the results of the present study show that the most favorable pilot ratings were for $\frac{\omega_\varphi}{\omega_{DR}}$ at or near unity, regardless of the magnitude of $\left|\frac{\varphi}{\beta}\right|$. Results reported in reference 2 for $\left|\frac{\varphi}{\beta}\right| = 8.05$ to 9.34 (see fig. 5) indicated a strong influence of the high $\left|\frac{\varphi}{\beta}\right|$ ratio, in that the most favorable pilot ratings were given for values of $\frac{\omega_\varphi}{\omega_{DR}}$ appreciably less than 1. It is believed that the results of reference 2 have been superseded by the results of the subject investigation and that of reference 3.

Comparison With Related Tests in a T-33 Variable-Stability Airplane

The results of the three-degree-of-freedom contact-analog simulation are compared with the results (ref. 3) obtained with the T-33 variable-stability airplane. In reference 3 the T-33 airplane was used as a ground and a flight simulator. The characteristics of the contact analog and the T-33 simulations are compared in the tabulation on page 21.

Figures 11 to 13 are plots of pilot rating versus $\frac{\omega_\varphi}{\omega_{DR}}$ obtained with the three methods of simulation. For the T-33 simulations the curves represent composite ratings obtained from reference 3. The composite pilot ratings are defined in reference 3 as being determined by the analyst after a detailed examination of the pilot comments for each evaluation and the pilot ratings for evaluations of maneuvers with and without random disturbances. The ratings shown for the contact analog represent an average rating for the two pilots.

In general, there is good agreement between the results obtained with the ground and in-flight simulators. Both the trend and the absolute value of the pilot rating showed fairly good agreement over the range of $\frac{\omega_\varphi}{\omega_{DR}}$ investigated at each of the values of $\left|\frac{\varphi}{\beta}\right|$.

SIMILARITIES AND DIFFERENCES OF SIMULATORS

Topic	Contact analog	T-33 airplane	
		Fixed base	In flight
Equations of motion	Three-degree-of-freedom lateral-directional equations of motion provided by an analog computer	Five-degree-of-freedom lateral-directional plus reference longitudinal short-period dynamics Velocity constant Aircraft motion calculated by an analog computer, feeding angle of attack, angle of sideslip, pitch, roll, and yaw rates to T-33 response feedback system	Five-degree-of-freedom lateral-directional plus reference longitudinal short-period dynamics Velocity constant Aircraft motion sensed in flight by angle-of-attack and angle-of-sideslip vanes Pitch, roll, and yaw rates sensed by means of rate gyros Sensed quantities fed to T-33 response feedback gains calibrated to provide desired simulated dynamics
Pilot cues	Visual—pseudo-outside world display generated by an analog computer No cockpit motions	Airplane instruments mechanized by an analog computer No cockpit motions	Visual—outside world plus aircraft instruments Cockpit motion represented realistically
Cockpit control feel system	Aileron stick and rudder pedals available Control force linearly proportional to deflection Force feel provided by bungees	Elevator and aileron stick and rudder pedals fly-by-wire systems connected to their respective electrohydraulic actuators	
Evaluation task	As specified on page 9	As specified on page 9, plus evaluation with random disturbance	

For $\left|\frac{\varphi}{\beta}\right| < 1.0$ and $\frac{\omega_\varphi}{\omega_{DR}} > 1.0$ (fig. 11) the in-flight simulation shows more favorable ratings than shown by either the contact analog or the T-33 ground simulation. The motion and visual cues may account for the pilot's increased confidence in assessing the predominant Dutch roll oscillation problem.

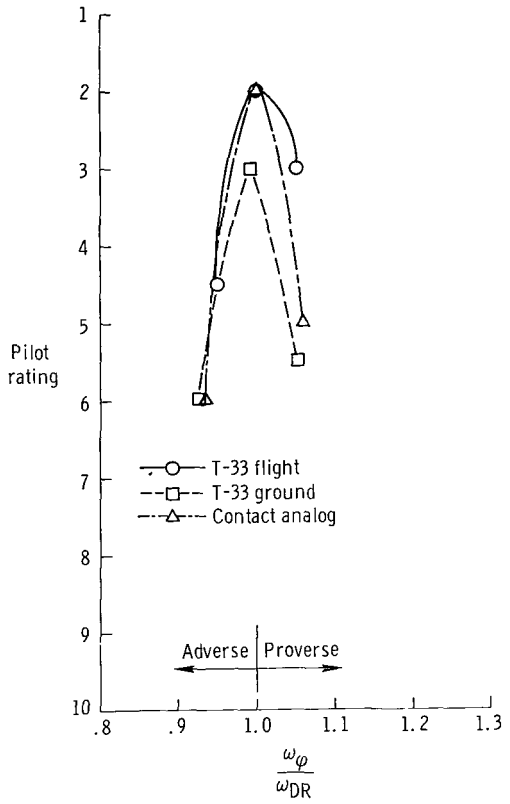

Figure 11.– Comparison of the results obtained with ground and in-flight simulators for $\left|\frac{\varphi}{\beta}\right| < 1.0$.

For $\left|\frac{\varphi}{\beta}\right| \approx 9.2$ (fig. 12) the trends in pilot rating show fairly good agreement between the three methods of simulation. The pilot opinion trends show that the pilots do not like large yaw due to aileron, either adverse or proverse. The most favorable ratings were for $\frac{\omega_\varphi}{\omega_{DR}} = 1.0$ and minimum sideslip excitation, i.e., a condition approaching the ideal one-degree-of-freedom roll response.

For $\left|\frac{\varphi}{\beta}\right| \approx 13.0$ (fig. 13) the overall results again showed a pilot preference for $\frac{\omega_\varphi}{\omega_{DR}}$ near unity. The T-33 ground simulation results showed consistently less favorable ratings, for equivalent values of $\frac{\omega_\varphi}{\omega_{DR}}$, than the T-33 flight and the contact-analog simulations. A plausible explanation is the decrease in roll damping of the T-33 ground simulation noted by the pilots and verified in the subsequent analysis of the data. The decrease in roll damping affected the control of closed-loop roll oscillations. The curve representing the contact-analog results showed a better overall rating for proverse yaw values than either the T-33 ground or flight simulation. It should be noted that the T-33 simulations included random disturbances, whereas the contact analog did not. The random disturbances were taken into account in arriving at the composite pilot ratings. The disturbances tended to downrate a configuration with high effective dihedral.

Less tangible, but believed to be a factor in the evaluation, were the pilot's cues, motion and visual. The best pilot cues were found in the T-33 in-flight simulation, in which motion and visual (outside-world reference) cues were realistic. The realism of the simulation gave the evaluation pilot added confidence in assessing a configuration. The contact analog offered a pseudo-outside world visual display. Although cockpit instruments were also available, the pilots used the contact-analog display a large

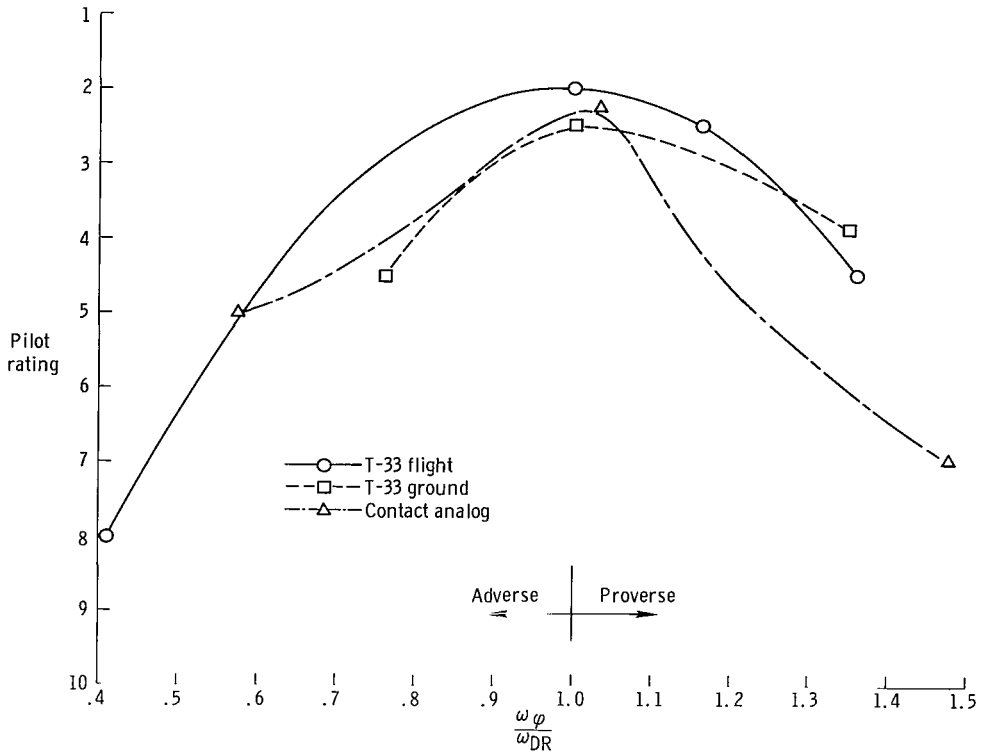

Figure 12.– Comparison of the results obtained with ground and in-flight simulators for $\left|\frac{\varphi}{\beta}\right| \approx 9.2$.

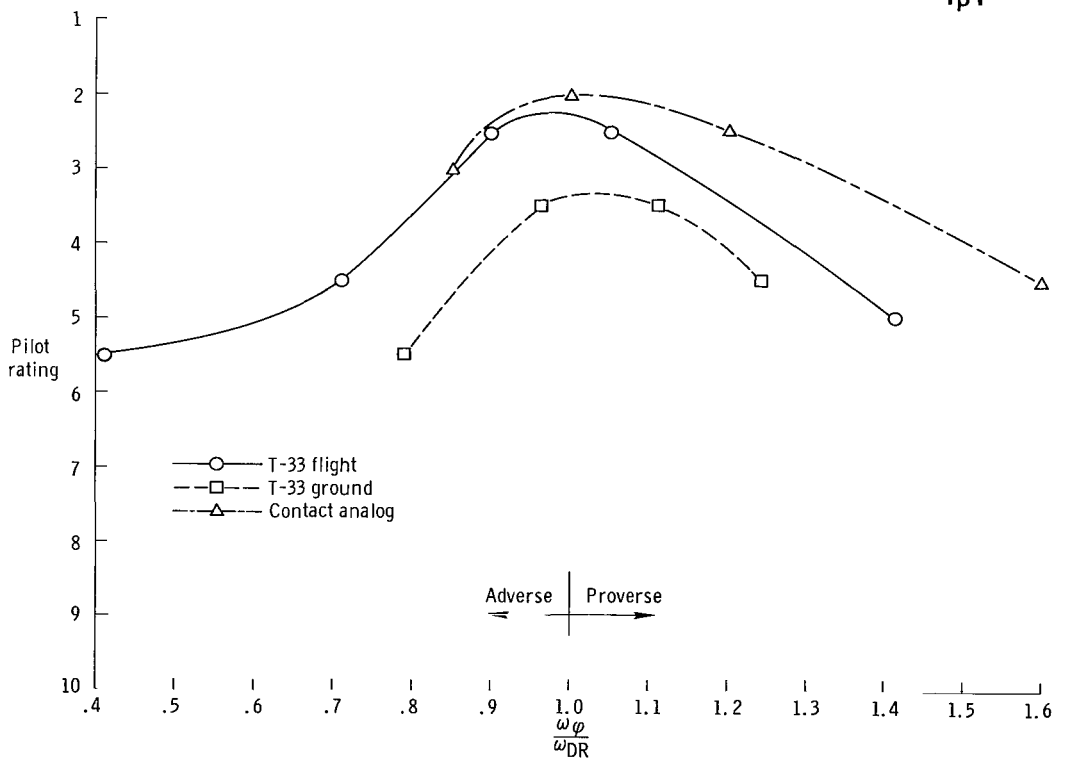

Figure 13.– Comparison of the results obtained with ground and in-flight simulators for $\left|\frac{\varphi}{\beta}\right| \approx 13.0$.

percentage of the time. The T-33 ground simulation relied on cockpit instruments only, as in simulated Instrument Flight Rules (IFR) flight. Since the human pilot is adaptable to the task at hand, it is difficult to quantitatively evaluate the effect on the results of this study caused by differences between displays.

As shown in the tabulation on page 8, the contact-analog simulation had a maximum stick displacement of ±3.00 inches (±7.62 centimeters) and a force gradient of 4.67 lb/in. (0.834 kg/cm), whereas the corresponding values for the T-33 were ±6.00 inches (±15.25 centimeters) and 2.3 lb/in. (0.410 kg/cm). The compensating factor was the aileron gearing; the T-33 simulation had twice the value of the contact analog. Thus, the unit force displacement was not matched, but the response per unit deflection was. It is believed that the difference in force displacement per unit deflection of the aileron stick did not influence the evaluation of the simulation.

Remarks on Pilot Techniques

In normal flight the Dutch roll oscillation in itself is not the pilot's primary concern but, rather, a side effect of his efforts to control the airplane in some other mode of response and, as such, falls into the category of a nuisance he has to cope with. In the fixed-base simulation the primary piloting task was to evaluate the lateral controllability of the various configurations; thus, the pilot evaluated the effect of his control on the airplane response. Several techniques were used by the pilots to control the configurations.

A $\dot{\beta}$ technique was effective for controlling flight conditions identified with adverse yaw and small $\left|\frac{\varphi}{\beta}\right|$ ratios. The technique consisted of applying sharp aileron stick pulses in the direction of the airplane yaw at the precise time of zero sideslip angle. At that same instant, sideslip rate $\dot{\beta}$ was at its maximum value. This technique, useful for emergency operation, was very demanding and required split-second execution. Three to four aileron-pulse applications usually damped the oscillation.

The rudders were successfully used to damp out the oscillations when the condition had adverse yaw and low $\left|\frac{\varphi}{\beta}\right|$ ratio. For high $\left|\frac{\varphi}{\beta}\right|$ and proverse aileron yaw configurations, the pilots were generally not inclined to use rudders for coordination or damping.

Pilot-induced oscillations were experienced at the larger values of proverse aileron yaw associated with large $\left|\frac{\varphi}{\beta}\right|$. The favored control method was to use ailerons only and to maneuver the airplane as slowly as possible to minimize roll and Dutch roll excitation. Roll oscillations could be damped with aileron pulses; however, ailerons were not effective for damping Dutch roll oscillations. The oscillations did subside in time, in a controls-fixed condition.

CONCLUSIONS

A three-degree-of-freedom fixed-base contact-analog simulation study of the lateral-directional handling qualities of piloted reentry vehicles established that:

1. The pilots preferred the ratio of the roll transfer function numerator frequency to the Dutch roll frequency to be unity, independent of the magnitude of bank angle to sideslip angle ratio, which was evaluated at values of 0.67, 9.2, and 13.0.

2. The pilots objected to the excessive amount of sideslip-angle excitation with ailerons when the ratio of the roll transfer function numerator frequency to Dutch roll frequency was different from unity, the bank angle to sideslip angle ratio was low, and the yawing moment due to aileron was large.

3. Large rolling-motion excursions were distracting to the pilots and led to miscoordination and pilot-induced oscillations. The combination of large bank angle to sideslip angle ratio and roll transfer function numerator frequency to Dutch roll frequency ratio greater than unity produced rolling-motion excursions that resulted from sideslip induced by ailerons.

4. The pilots preferred configurations approaching the ideal one-degree-of-freedom roll response; that is, a minimum of sideslip and bank-angle oscillation at Dutch roll frequencies induced by aileron control inputs.

5. There was good correlation between the results obtained with the three-degree-of-freedom contact-analog simulator and the results obtained during a concurrent study with a five-degree-of-freedom variable-stability T-33 airplane.

Flight Research Center,
National Aeronautics and Space Administration,
Edwards, Calif., September 6, 1967,
126-16-01-07-24.

APPENDIX A

COMPARISON OF THE EQUATIONS OF MOTION USED FOR THE IN-FLIGHT AND CONTACT-ANALOG SIMULATIONS

The lateral-directional equations of motion used in the T-33 simulation are compared with the equations used for the mechanization of the contact-analog simulation. These equations are valid for small perturbations about the stability axes.

The equations of motion (appendix A, ref. 3) used for the T-33 simulation were as follows:

$$\begin{bmatrix} \left(Y_\beta - s\right) & -1 & \frac{g}{V} \\ \left(N'_\beta + N'_{\dot\beta}s\right) & \left(N'_r - s\right) & N'_p s \\ \left(L'_\beta + L'_{\dot\beta}s\right) & L'_r & \left(L'_p - s\right)s \end{bmatrix} \begin{bmatrix} \beta \\ r \\ \varphi \end{bmatrix} = \begin{bmatrix} -Y_{\delta_{a_s}} & -Y_{\delta_{r_p}} \\ -N'_{\delta_{a_s}} & -N'_{\delta_{r_p}} \\ -L'_{\delta_{a_s}} & -L'_{\delta_{r_p}} \end{bmatrix} \begin{bmatrix} \delta_{a_s} \\ \delta_{r_p} \end{bmatrix} \tag{A1}$$

For the contact-analog study the following equations of motion were used:

$$\begin{bmatrix} \left(Y_\beta - s\right) & -1 & \frac{g}{V} \\ N'_\beta & \left(N'_r - s\right) & N'_p s \\ L'_\beta & L'_r & \left(L'_p - s\right)s \end{bmatrix} \begin{bmatrix} \beta \\ r \\ \varphi \end{bmatrix} = \begin{bmatrix} 0 & 0 \\ -N'_{\delta_{a_s}} & -N'_{\delta_{r_p}} \\ -L'_{\delta_{a_s}} & -L'_{\delta_{r_p}} \end{bmatrix} \begin{bmatrix} \delta_{a_s} \\ \delta_{r_p} \end{bmatrix} \tag{A2}$$

In comparing the above equations term by term, it can be seen that:

1. $Y_{\delta_{a_s}}$ and $Y_{\delta_{r_p}}$ in equation (A1) were omitted from equation (A2), $Y_{\delta_{a_s}}$ was negligibly small, and $Y_{\delta_{r_p}}$ was of minor significance.

2. $N'_{\dot\beta}s$ from equation (A1) was omitted from equation (A2). This omission was compensated for by adding the appropriate increment of $\left|N'_{\dot\beta}\right|$ to N'_r of equation (A2).

3. $L'_{\dot\beta}s$ from equation (A1) was omitted from equation (A2). This omission was compensated for by adding the appropriate increment of $\left|L'_{\dot\beta}\right|$ to L'_r of equation (A2).

By comparing the lateral-directional dynamic modes, such as τ_s, τ_r, ω_φ, ζ_φ, ω_{DR}, and ζ_{DR}, of the contact-analog simulation (see table on page 11) with those of

the T-33 simulations (tables I-1, I-2, I-3, and I-4 of ref. 3), it can be seen that small variations existed. These variations are accepted as an inherent characteristic of a variable-stability airplane equipped with a response feedback system, such as the T-33.

APPENDIX B

SIMPLIFICATIONS OF THE EQUATIONS OF MOTION

The objectives of this study were to assess the influence of pilot opinion caused by controlled changes in lateral-directional parameters. A derivation of the equations for these parameters and their simplification was as follows:

$$\begin{bmatrix} (Y_\beta - s) & -1 & \frac{g}{V} \\ N'_\beta & (N'_r - s) & N'_p s \\ L'_\beta & L'_r & (L'_p - s)s \end{bmatrix} \begin{bmatrix} \beta \\ r \\ \varphi \end{bmatrix} = \begin{bmatrix} 0 & 0 \\ -N'_{\delta_{a_s}} & -N'_{\delta_{r_p}} \\ -L'_{\delta_{a_s}} & -L'_{\delta_{r_p}} \end{bmatrix} \begin{bmatrix} \delta_{a_s} \\ \delta_{r_p} \end{bmatrix} \tag{B1}$$

The bank angle per aileron stick transfer function can be written as follows:

$$\frac{\varphi(s)}{\delta_{a_s}(s)} = \frac{1}{\Delta}\left[+L'_{\delta_{a_s}}s^2 + \left(-Y_\beta L'_{\delta_{a_s}} - N'_r L'_{\delta_{a_s}} - N'_{\delta_{a_s}} L'_r\right)s + L'_{\delta_{a_s}} Y_\beta N'_r - L'_\beta N'_{\delta_{a_s}} - Y_\beta L'_r N'_{\delta_{a_s}} - N'_\beta L'_{\delta_{a_s}}\right] \tag{B2}$$

where Δ is the denominator.

Then

$$\Delta = +s^4 + \left(-Y_\beta - N'_r - L'_p\right)s^3 + \left(+N'_r Y_\beta + Y_\beta L'_p + N'_r L'_p + N'_\beta - L'_r N'_p\right)s^2 + \left(-Y_\beta N'_r L'_p + L'_\beta N'_p - L'_\beta \frac{g}{V} - N'_\beta L'_p + Y_\beta L'_r N'_p\right)s + \frac{g}{V}\left(-N'_\beta L'_r + N'_r L'_\beta\right) \tag{B3}$$

The transfer function may be written in modal form as

$$\frac{\varphi(s)}{\delta_{a_s}(s)} = \frac{L'_{\delta_{a_s}}\left(s^2 + 2\zeta_\varphi \omega_\varphi s + \omega_\varphi{}^2\right)}{\left(s + \frac{1}{\tau_s}\right)\left(s + \frac{1}{\tau_r}\right)\left(s^2 + 2\zeta_{DR}\omega_{DR}s + \omega_{DR}{}^2\right)} \tag{B4}$$

Multiplying the denominator gives

$$\Delta = s^4 + \left(\frac{1}{\tau_s} + \frac{1}{\tau_r} + 2\zeta_{DR}\omega_{DR}\right)s^3 + \left[\frac{1}{\tau_s\tau_r} + 2\zeta_{DR}\omega_{DR}\left(\frac{1}{\tau_s} + \frac{1}{\tau_r}\right) + \omega_{DR}{}^2\right]s^2 + \left[\omega_{DR}{}^2\left(\frac{1}{\tau_s} + \frac{1}{\tau_r}\right) + \frac{2\zeta_{DR}\omega_{DR}}{\tau_s\tau_r}\right]s + \frac{\omega_{DR}{}^2}{\tau_s\tau_r} \tag{B5}$$

Since the pilots never observed the effects of the spiral mode, it will be assumed that its effect was neutral, i.e., $\frac{1}{\tau_s} \approx 0$. Thus, rewriting equation (B5) results in the following expression:

$$\Delta \approx s\left[s^3 + \left(2\zeta_{DR}\omega_{DR} + \frac{1}{\tau_r}\right)s^2 + \left(\omega_{DR}^2 + \frac{2\zeta_{DR}\omega_{DR}}{\tau_r}\right)s + \frac{\omega_{DR}^2}{\tau_r}\right]$$

Also, assuming $\frac{g}{V} \approx 0$ equation (B3) becomes

$$\Delta \approx s\left[s^3 - \left(Y_\beta + N'_r + L'_p\right)s^2 + \left(N'_r Y_\beta + Y_\beta L'_p + N'_r L'_p + N'_\beta - L'_r N'_p\right)s + \left(L'_\beta N'_p - Y'_\beta N'_r L'_p - N'_\beta L'_p + Y_\beta L'_r N'_p\right)\right] \quad \text{(B6)}$$

where

$$2\zeta_{DR}\omega_{DR} + \frac{1}{\tau_r} \approx -\left(Y_\beta + N'_r + L'_p\right) \quad \text{(B7)}$$

and

$$\frac{\omega_{DR}^2}{\tau_r} \approx L'_\beta N'_p - Y'_\beta N'_r L'_p - N'_\beta L'_p + Y_\beta L'_r N'_p \quad \text{(B8)}$$

For the additional assumption that the roll-mode time constant $\frac{1}{\tau_r} \approx -L'_p$, equations (B7) and (B8) become

$$\begin{aligned} 2\zeta_{DR}\omega_{DR} &\approx -Y_\beta - N'_r \\ \omega_{DR}^2 &\approx \frac{-L'_\beta N'_p}{L'_p} + N'_\beta + Y_\beta\left(\frac{-L'_r N'_p}{L'_p} + N'_r\right) \end{aligned} \quad \text{(B9)}$$

or

$$\omega_{DR}^2 \approx N'_\beta + N'_r Y_\beta - \frac{N'_p}{L'_p}\left(Y_\beta L'_r + L'_\beta\right) \quad \text{(B10)}$$

Comparing the numerator in modal and derivative form, equations (B4) and (B2), simplify to

$$L'_{\delta_{a_s}}\left(s^2 + 2\zeta_\varphi\omega_\varphi s + \omega_\varphi^2\right) = L'_{\delta_{a_s}}s^2 + s\left(-Y_\beta L'_{\delta_{a_s}} - N'_r L'_{\delta_{a_s}} + N'_{\delta_{a_s}} L'_r\right) + L'_{\delta_{a_s}} Y_\beta N'_r - L'_\beta N'_{\delta_{a_s}} - Y_\beta L'_r N'_{\delta_{a_s}} + N'_\beta L'_{\delta_{a_s}} \quad \text{(B11)}$$

The predominant modes are

$$2\zeta_\varphi\omega_\varphi = -N'_r - Y_\beta + \frac{N'_{\delta_{a_S}}}{L'_{\delta_{a_S}}} L'_r \tag{B12}$$

and

$$\omega_\varphi{}^2 = Y_\beta N'_r + N'_\beta - \frac{N'_{\delta_{a_S}}}{L'_{\delta_{a_S}}} \left(L'_\beta + Y_\beta L'_r\right) \tag{B13}$$

Taking the ratio of equation (B13) over equation (B10) results in

$$\left(\frac{\omega_\varphi}{\omega_{DR}}\right)^2 = \frac{Y_\beta N'_r + N'_\beta - \frac{N'_{\delta_{a_S}}}{L'_{\delta_{a_S}}}\left(L'_\beta + Y_\beta L'_r\right)}{N'_\beta + N'_r Y_\beta - \frac{N'_p}{L'_p}\left(Y_\beta L'_r + L'_\beta\right)} \tag{B14}$$

For the additional assumption of $Y_\beta = N'_p = 0$

$$\left(\frac{\omega_\varphi}{\omega_{DR}}\right)^2 = \frac{N'_\beta - \frac{N'_{\delta_{a_S}}}{L'_{\delta_{a_S}}} L'_\beta}{N'_\beta} = 1 - \frac{N'_{\delta_{a_S}}}{L'_{\delta_{a_S}}} \frac{L'_\beta}{N'_\beta} \tag{B15}$$

As can be seen, from the preceding derivation, equation (B15) is simplified. Nevertheless, it represents the primary derivatives for the $\frac{\omega_\varphi}{\omega_{DR}}$ ratio. This simplified expression for $\frac{\omega_\varphi}{\omega_{DR}}$ was presented in the text (page 16) for the purpose of discussion only.

Derivation of the steady-state roll rate per aileron stick open-loop transfer function for a neutral spiral mode (i.e., $\frac{1}{\tau_S} \approx 0$) from equation (B4) becomes

$$\frac{\varphi}{\delta_{a_S}}(s) = \frac{L'_{\delta_{a_S}}\left(s^2 + 2\zeta_\varphi\omega_\varphi s + \omega_\varphi{}^2\right)}{s\left(s + \frac{1}{\tau_r}\right)\left(s^2 + 2\zeta_{DR}\omega_{DR}s + \omega_{DR}{}^2\right)} \tag{B16}$$

and

$$\frac{\dot{\varphi}}{\delta_{a_s}}(s) = \frac{p}{\delta_{a_s}}(s) = \frac{L'_{\delta_{a_s}} \omega_\varphi^2}{\left(\omega_{DR}^2 s + \frac{\omega_{DR}^2}{\tau_r}\right)} \left[\frac{\frac{s^2}{\omega_\varphi^2} + \frac{2\zeta_\varphi}{\omega_\varphi} s + 1}{\frac{s^2}{\omega_{DR}^2} + \frac{2\zeta_{DR}}{\omega_{DR}} s + 1}\right] \tag{B17}$$

In order to find the steady-state value in real time at time $t = \infty$, the final value theorem is used where $\lim_{t \to \infty} f(t) = \lim_{s \to 0} sF(s)$; hence, equation (B17) becomes

$$\left.\frac{p}{\delta_{a_s}}(t)\right|_{t=\infty} = L'_{\delta_{a_s}} \tau_r \left(\frac{\omega_\varphi}{\omega_{DR}}\right)^2 \tag{B18}$$

which is the steady-state roll rate per aileron stick step input.

REFERENCES

1. Ashkenas, Irving L.; and McRuer, Duane T.: The Determination of Lateral Handling Quality Requirements From Airframe-Human Pilot System Studies. Tech. Rep. 59-135, Wright Air Dev. Center, U.S. Air Force, June 1959.

2. Harper, Robert P., Jr.: In-Flight Simulation of the Lateral-Directional Handling Qualities of Entry Vehicles. Tech. Rep. 61-147, Wright Air Dev. Div., U.S. Air Force, Nov. 1961.

3. Meeker, J. I.: Evaluation of Lateral-Directional Handling Qualities of Piloted Re-entry Vehicles Utilizing Fixed-Base and In-Flight Evaluations. NASA CR-778, 1967.

4. Ball, J. N.: Installation of an Automatic Control System in a T-33 Airplane for Variable Stability Flight Research. Part 1 - Preliminary Investigation and Design Studies. TR 55-156, Wright Air Dev. Center, U.S. Air Force, Apr. 1955.

5. Flight Research Department: Installation of an Automatic Control System in a T-33 Airplane for Variable Stability Flight Research. Part 2. Detail Design, Fabrication and Installation. TR-55-156, Wright Air Dev. Center, U.S. Air Force, Sept. 1956.

6. Beilman, J. L.; and Harper, R. P., Jr.: Installation of an Automatic Control System in a T-33 Airplane for Variable Stability Flight Research. Part 3. Ground and Flight Checkout. TR 55-156, Wright Air Dev. Center, U.S. Air Force, Aug. 1957.

NASA-Langley, 1968 —— 31 H-482

National Aeronautics and Space Administration
WASHINGTON, D. C.

OFFICIAL BUSINESS

FIRST CLASS MAIL

POSTAGE AND FEES PAID
NATIONAL AERONAUTICS AND
SPACE ADMINISTRATION

12U 001 56 51 3DS 68074 00903
AIR FORCE WEAPONS LABORATORY/AFWL/
KIRTLAND AIR FORCE BASE, NEW MEXICO 87117

ATT MISS MADELINE F. CANOVA, CHIEF TECHNI
LIBRARY /WLIL/

POSTMASTER: If Undeliverable (Section 158 Postal Manual) Do Not Return

"The aeronautical and space activities of the United States shall be conducted so as to contribute . . . to the expansion of human knowledge of phenomena in the atmosphere and space. The Administration shall provide for the widest practicable and appropriate dissemination of information concerning its activities and the results thereof."

—NATIONAL AERONAUTICS AND SPACE ACT OF 1958

NASA SCIENTIFIC AND TECHNICAL PUBLICATIONS

TECHNICAL REPORTS: Scientific and technical information considered important, complete, and a lasting contribution to existing knowledge.

TECHNICAL NOTES: Information less broad in scope but nevertheless of importance as a contribution to existing knowledge.

TECHNICAL MEMORANDUMS: Information receiving limited distribution because of preliminary data, security classification, or other reasons.

CONTRACTOR REPORTS: Scientific and technical information generated under a NASA contract or grant and considered an important contribution to existing knowledge.

TECHNICAL TRANSLATIONS: Information published in a foreign language considered to merit NASA distribution in English.

SPECIAL PUBLICATIONS: Information derived from or of value to NASA activities. Publications include conference proceedings, monographs, data compilations, handbooks, sourcebooks, and special bibliographies.

TECHNOLOGY UTILIZATION PUBLICATIONS: Information on technology used by NASA that may be of particular interest in commercial and other non-aerospace applications. Publications include Tech Briefs, Technology Utilization Reports and Notes, and Technology Surveys.

Details on the availability of these publications may be obtained from:

SCIENTIFIC AND TECHNICAL INFORMATION DIVISION

NATIONAL AERONAUTICS AND SPACE ADMINISTRATION

Washington, D.C. 20546